ELSEVIER

Journal of Nuclear Materials 283–287 (2000) 518–522

journal of nuclear materials

www.elsevier.nl/locate/jnucmat

On the mechanisms and mechanics of fracture toughness of a V–4Cr–4Ti alloy

E.G. Donahue *, G.R. Odette, G.E. Lucas

Department of Mechanical and Environmental Engineering, University of California, Santa Barbara, CA 93106, USA

Abstract

Effects of irradiation and crossrolling on fracture toughness–temperature curves of the program heat of the V–4Cr–4Ti were evaluated. The alloy undergoes normal stress controlled cleavage fracture at low temperatures and ductile tearing fracture at higher temperature. It appears that crossrolling lowers the cleavage transition temperature. A critical stress–critical-stressed area cleavage criterion is used to model toughness–temperature curves in the cleavage transition, including the effect of specimen size. Irradiation induced increases in the transition temperature are accurately predicted by an equivalent yield stress model. Ductile tearing toughness is also degraded by irradiation, correlating with reduced uniform strains measured in tensile tests. Large cleavage transition temperature shifts and ductile toughness decreases may limit the application of V–4Cr–4Ti alloys for service in low-to-intermediate temperature irradiation environments.

1. Introduction

Vanadium alloys are one class of low-activation materials under consideration for fusion structures. As such, one of the properties of interest is their fracture toughness. The work reported here is part of an overall effort to develop physical models of the fracture toughness of a vanadium alloy to treat the effects of: (a) specimen/structure size and geometry; (b) loading rate; (c) metallurgical factors associated with processing and fabrication history; (d) irradiation embrittlement. Due to paper length limitations, the effects of specimen size, geometry and orientation will not be discussed here.

2. Experimental and data analysis procedures

Specimens were fabricated from the 500 kg program heat (#832665) of V–4Cr–4Ti manufactured by Teledyne Wah Chang [1]. The deformation processing and recrystallization heat treatments were carried out by ORNL [2]. Miniature, side-grooved (a total of 20%) 1/3 sized Charpy (MPCC) bars ($W = B = 3.3$ mm, $L = 17$ mm) were fabricated from the as rolled (6.35 mm thick) or as-crossrolled (3.8 mm thick) plate in the LT orientations (crack propagation perpendicular to the extrusion direction). The specimens were heat treated in vacuum at 1000°C for 2 h, and pre-cracked to $a/W \approx 0.5$ per ASTM E-399 [3]. One set of specimens was irradiated in the High Flux Beam Reactor (HFBR) to about 0.1 dpa at 160°C, 255°C, 295°C and 390°C, complementing previous studies of an irradiation to about 0.4 dpa at 200°C [4].

Fracture tests were conducted under displacement control at loading rates of 2.54 μm/s. Cleavage fracture occurred by load-shedding pop-ins. [1] In some cases maximum loads were observed prior to the pop-in.

* Corresponding author. Tel.: +1-805 893 3212; fax: +1-805 893 8651.

E-mail address: donahue@engineering.ucsb.edu (E.G. Donahue).

[1] A pop-in is defined as a sudden propagation and arrest of a cleavage crack along some fraction of the crack front. Pop-ins are relatively small and typically have a halfpenny-type shape. They are accompanied by a small rapid load drop. A residual load is sustained by the ligament upon further displacement. A pop-in contrasts to cleavage resulting in a complete or nearly complete, specimen break and very large load drop.

0022-3115/00/$ - see front matter
PII: S 0 0 2 2 - 3 1 1 5 (0 0) 0 0 2 2 8 - 2

Often the first pop-ins were small and were followed by additional deformation terminated by another pop-in. Thus, cleavage fracture was defined based on $\geqslant 5\%$ total load shedding. Cases with total pop-in load shedding less than 5% were deemed as provisional cleavage. In other cases pop-ins were not observed. In this case, ductile toughness was defined by the maximum load, K_{max}. Beyond maximum load, cracks extended either (a) by actual ductile tearing or sliding-off at the crack tip, probably associated with flow localization or (b) by continued blunting [5].

Consistent with the intrinsic statistical nature of cleavage in the transition [6], the toughness data are highly scattered. This scatter, coupled with the limited number of small specimens, makes it difficult to quantify subtle effects related to specimen size, processing history and orientation. Since the small specimen size also places severe constraints on the maximum elastic–plastic K_{Jc} toughness that can be measured [6], most data is for provisional (K_q) or effective toughness, K_e. Since the small specimens also did not permit J_R–Δa tests [7,8], ductile fracture was specified based on the maximum load.

The effective toughness (invalid K_q, valid K_{Jc} and K_{max}) data were evaluated with both 'standard' elastic–plastic fracture mechanics methods [9] and the confocal microscopy–fracture reconstruction (CM–FR) technique [10,11]. CM–FR is used to measure the critical crack tip opening displacement, δ_c, which is related to toughness as $J_{q/Ic} \approx 2\sigma_y\delta_c$, where σ_y is the yield stress [12–14]. Good consistency was observed between the alternate methods of evaluating toughness. All results are represented as an effective toughness, $K_{q/Jc} = K_e = (J_{q/Ic}E')^{1/2}$, where E' is the plane strain modulus.

CM–FR was also used to characterize the sequence and locations of local material separation events (e.g., cleavage facets, microvoids, decohesion zones) in the process zone of the blunting crack tip [10,11]. Scanning electron microscopy (SEM) was used to characterize the local fracture mode and features, initiation sites and fracture surface deformation patterns.

The unirradiated K_e data were constraint corrected to provide estimates of K_{Jc} based on a critical stress (σ^*)–critical area (A^*) local fracture model. Details of this model are described elsewhere [5,15,16]. Briefly, however, finite element method (FEM) calculations were used to simulate crack tip fields as a function of the alloy constitutive law [17], specimen size and geometry and the applied load and displacement. The model assumes cleavage fracture occurs when a critical stress contour (σ^*) encompasses a critical area (A^*) at a critical δ_c or K_e. Thus σ^*–A^* are the actual measures of material toughness that specify local conditions for cleavage crack advance, hence, $K_{Jc}(T)$. It is assumed that the σ^*–A^* criteria are independent of temperature. In the limiting case of small scale yielding (SSY) the $K_{Jc}(T)$ curve is unique. More generally, $K_e(T)$ depends specifically on the specimen geometry and deformation level ($D = K_e^2/\sigma_y(W-a)$). Constraint corrections are based on FEM calculations of the K_e/K_{Jc}-ratio needed to produce the same σ^*–A^*. For a given geometry and constitutive law, K_e/K_{Jc} is a function of only D and σ^*/σ_y.

Irradiation (ϕt) and loading rate (P') induced shifts in the cleavage transition temperatures ($\Delta T_{\phi t/P'}$) were compared to predictions of the equivalent yield stress model (EYSM) [18]. The EYSM postulates that the toughness at a reference value after irradiation or at a high loading rate, occurs at a temperature ($\Delta T_{\phi t,P'}$) corresponding to the same yield stress, $\sigma_y(\Delta T_{\phi t/P'})$, as the yield stress, $\sigma_y(T_{or})$, at the temperature corresponding to the reference toughness in the unirradiated condition at the reference strain rate or $\sigma_y(T_{\phi t,P'} = \sigma_y(T_{or})$. A key assumption is that σ^* (and by implication A^*) is independent of irradiation, loading rate and temperature. Thus, yield stress elevations ($\Delta\sigma_y$) increase the temperature at the reference toughness as $\Delta T_{\phi t,P'} = T_{\phi t,P'} - T_{or} = \Delta\sigma_y/\langle d\sigma_y/dT\rangle$, where $\langle d\sigma_y/dT\rangle$ is averaged over the temperature shift interval.

A previously published decohesion model for irradiated stainless steels [19], proposes that ductile toughness crudely correlates with a combination of yield stress (σ_y), ultimate stress (σ_u), and uniform strain (ε_u) tensile properties as defined by a irradiated (i) to unirradiated (u) toughness ratio parameter, $R = K_i/K_u = \{[(\sigma_{yi}+\sigma_{ui})/(\sigma_{yu}+\sigma_{uu})](\varepsilon_{ui}/\varepsilon_{uu})\}^{1/2}$. Trends in the observed K_{max} versus R are also reported.

3. Results

Fig. 1 shows toughness data from MPCC tests from rolled versus crossrolled plate in the LT orientation. The

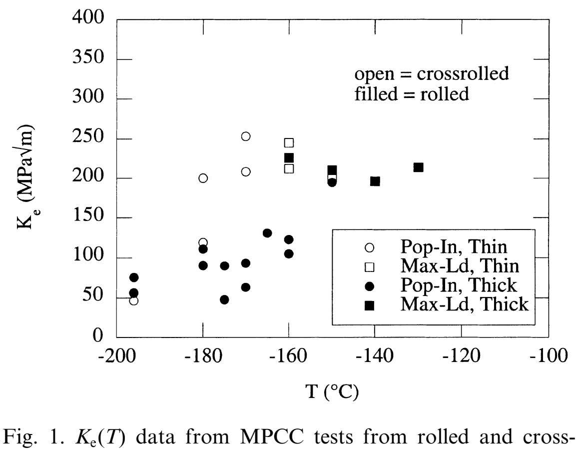

Fig. 1. $K_e(T)$ data from MPCC tests from rolled and crossrolled plate. Both sets of specimens were in the LT orientation with respect to the extrusion direction. The crossrolled material exhibited higher toughness associated with a downward shift in the $K_e(T)$ curve.

crossrolled material exhibited higher toughness associated with a downward shift of $K_e(T)$ data by about 20°C. The K_e data (open symbols) corrected to SSY K_{Jc} (filled symbols) assuming $\sigma^*/\sigma_y = 3$ are shown in Fig. 2. Fig. 2 also shows the corresponding SSY $K_{Jc}(T)$ curves predicted by the σ^*–A^* model for both the rolled and crossrolled plates for $A^* = 10^{-8}$ m^2 and σ^* 1750 MPa (rolled) and 1900 MPa (crossrolled).

Since σ_y increases with increasing strain rate [20], higher loading rates shift $K_e(T)$ curves to higher temperatures [21]. As reported previously, measured shifts associated with rate increases by factors of 10^5 (low dynamic) and 10^6 (intermediate-dynamic) were about 60°C and 70°C, respectively. Low-intermediate temperature irradiation also results in increases in σ_y, even at low dose [4,22]. Previously reported data for irradiation to ~0.4 dpa at 200°C [22] show a shift of about 165°C with a corresponding $\Delta\sigma_y \approx 330$ MPa [24]. As discussed in more detail elsewhere [21], CM–FR and SEM showed that irradiated and unirradiated cleavage fracture surfaces and processes were generally similar. However, there was evidence of irradiation enhanced flow localization in the form of frequent coarse slip steps. The irradiated K_{max} toughness of ($\approx$90 MPa $\sqrt{\text{m}}$) was much lower than that for the unirradiated material and, in contrast to the blunting-only behavior in the latter case, involved tearing and sliding-off along slip bands of highly concentrated deformation. Indeed, in some cases, the cleavage toughness was higher than the K_{max}.

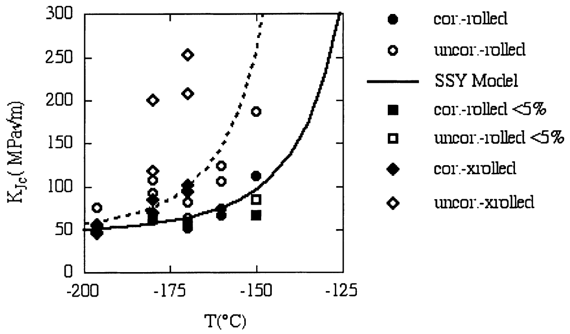

Fig. 2. Constraint correction to K_{Jc} data for each MPCC specimen, and the SSY $K_{Jc}(T)$ curves for both plate conditions, rolled (solid) and crossrolled (dashed). The σ^*–A^* criteria used for each condition differed slightly which accounts for the difference in SSY $K_{Jc}(T)$ curves.

Figs. 3(a) and (b) plot $K_e(T)$ data for irradiation to ~0.1 dpa at 160°C and 255°C, showing larger reductions in the K_{max}. CM–FR and SEM studies also indicated more pronounced tearing and crack sliding-off. Elevations of the cleavage transition temperature are also observed. However, since the maximum load and cleavage toughness are of the same order, only about 60 ± 20 MPa $\sqrt{\text{m}}$ for irradiation at 160°C, it is difficult to define a cleavage transition temperature shift. As shown in Figs. 3(c) and (d), the reductions in K_{max} are smaller for higher irradiation temperatures of 295°C and 390°C, and the increases in the cleavage transition temperature more obvious.

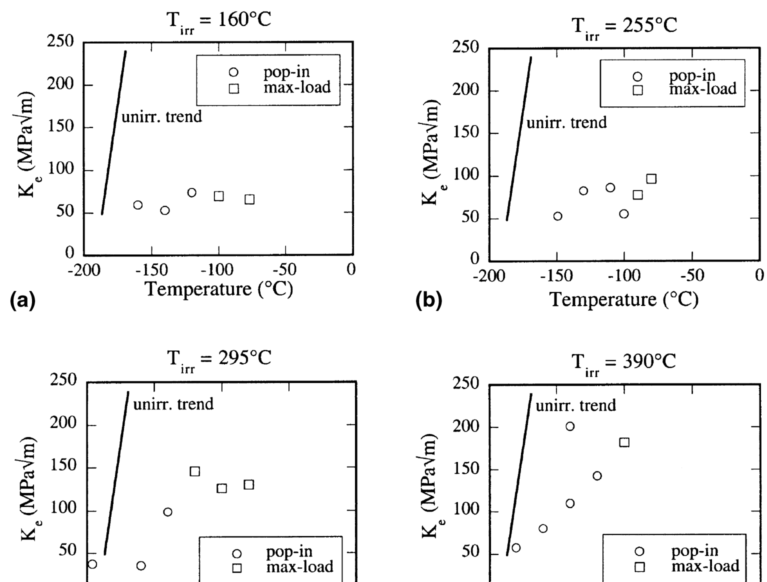

Fig. 3. $K_e(T)$ data for side-grooved MPCC specimens irradiated to 0.1 dpa at (a) 160°C, (b) 255°C, (c) 295°C and (d) 390°C.

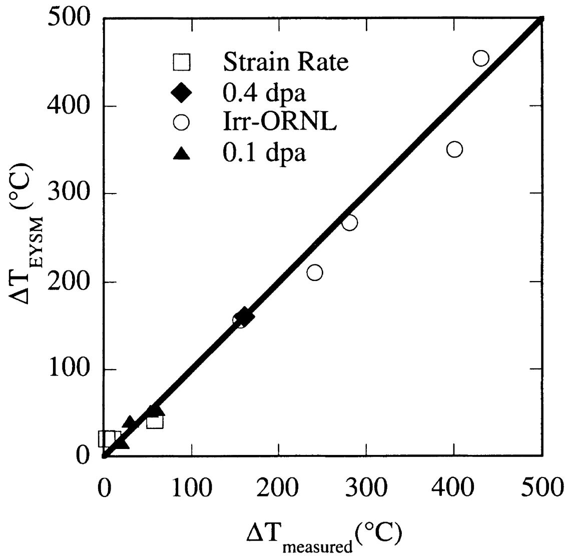

Fig. 4. Comparison of measured values of ΔT and values predicted by the EYSM.

Fig. 4 shows that the measured shifts in cleavage transition temperature ($\Delta T_{\phi t,P'}$) due to irradiation and loading rate are in excellent agreement with predictions of the EYSM and the corresponding elevations in σ_y ($\Delta\sigma_y$). For the 0.1 dpa irradiations, the $\Delta\sigma_y$ (MPa) $\approx$ 115 (390°C); 160 (295°C); 185 (255°C); and 130 (160°C). Fig. 4 also includes results from Alexander et al. [22]. The apparent success of the EYSM in predicting cleavage transition temperature shifts is somewhat puzzling in view of the increased flow localization after irradiation. Of course, flow localization has a more direct and profound effect on K_{max}, and the basic mode of fracture may change from classical microvoid coalescence to shear band decohesion associated with very fine scale damage in localized regions of very high strain [25]. Fig. 5 shows that the values of K_{max} for the irradiated material versus the toughness ratio, R, based on tensile data from the literature [4,23] and K_{max} for the unirradiated material are consistent with the predicted trend from the model, i.e., $K_i = R \cdot K_u$ [19]. The dominant effect of irradiation on K_{max} is associated with reductions in the uniform strain (ε_u) from $\varepsilon_{uu} \approx 0.15$ to ε_{ui} less than 0.01. Another puzzling observation, that the 0.1 dpa irradiations from 160°C to 250°C produce similar or even larger reductions in K_{max} than irradiation to 0.4 dpa at 200°C, is also qualitatively consistent with the competing effects of ε_{ui} and $\sigma_{y/ui}$ on R. The tensile data show that ε_{ui} decreases with dose more rapidly than the corresponding increases in $\sigma_{y/ui}$.

4. Summary and conclusions

The as-fabricated cleavage transition temperature of this vanadium alloy is low due to its low strength (e.g.,

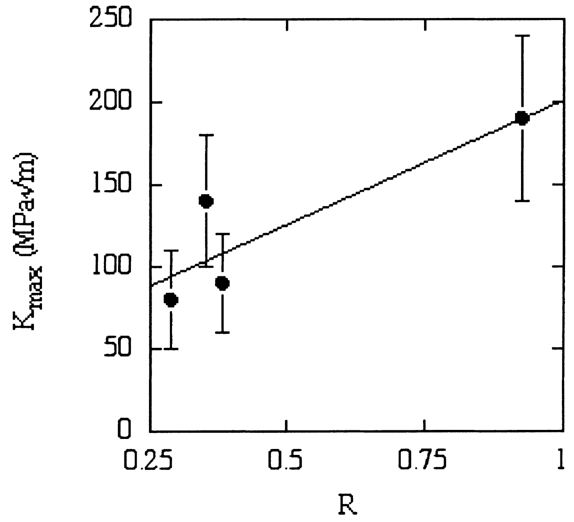

Fig. 5. Variations of K_{max} for irradiated material with the toughness ratio R. The line is given by $K_i = R \cdot K_u$. The data points represent measured values of K_i and values of the corresponding R determined from tensile data in the literature [4,23].

smaller than typical steels) combined with a high σ^* (comparable to steels). The effect of low strength on toughness is amplified in small specimens by the loss of triaxial constraint. A micromechanical model based on a critical stress–critical-stressed area, σ^*–A^*, cleavage criteria provides a basis for predicting $K_e(T)$ curves in the cleavage transition, including the effects of size pertinent to the use of small specimen data. Crossrolling lowers the transition temperature by increasing σ^*.

Irradiation and high loading rates result in upward shifts in the cleavage transition temperature, primarily due to corresponding increases in σ_y, as predicted by the EYSM. The low strain hardening and uniform strain observed in irradiated alloys produce even more profound degradation of K_{max}. The trends in the experimental estimates of K_{max} are qualitatively consistent with a simple model based on effects of irradiation on the tensile properties, as dominated by reductions in uniform strain.

The large cleavage transition temperature shifts and ductile toughness decreases may limit the application of V–4Cr–4Ti alloys in low-to-intermediate temperature irradiation environments.

Acknowledgements

The authors gratefully acknowledge the assistance of J.W. Sheckherd, D. Gragg and D. Klingensmith as well as that of our collaborators Arthur Rowcliffe and his colleagues at ORNL. The work was supported by the

US Department of Energy Grant # DE-FG03-87ER-52143.

References

[1] H.M. Chung, H.C. Tsai, D.L. Smith, R. Peterson, C. Curtis, C. Wojcik, R. Kinney, DOE/ER-0313/17, US Department of Energy, 1994, p. 178.
[2] A.N. Gubbi, A.F. Rowcliffe, D.J. Alexander, M.L. Grossbeck, W.S. Eatherly, DOE/ER-0313/18, US Department of Energy, 1995, p. 203.
[3] ASTM E399-90, in: Annual Book of ASTM Standards, American Society for Testing and Materials, 1996, p. 407.
[4] L.L. Snead, S.J. Zinkle, D.J. Alexander, A.F. Rowcliffe, J.P. Robertson, W.S. Eatherly, DOE/ER-0313/23, 1997, p. 81.
[5] G.R. Odette, K. Edsinger, G.E. Lucas, E. Donahue, in: Small Specimen Test Techniques, ASTM STP-1329, American Society for Testing and Materials, 1998.
[6] K. Wallin, T. Saario, K. Törrönen, Met. Sci. 18 (1984) 13.
[7] T.L. Anderson, R.H. Dodds Jr., J. Evaluation Testing 19 (2) (1991) 123.
[8] ASTM E1152-95, in: Annual Book of ASTM Standards, American Society for Testing and Materials, 1996, p. 750.
[9] ASTM E813-89, in: Annual Book of ASTM Standards, American Society for Testing and Materials, 1996, 633.
[10] K. Edsinger, PhD thesis, Department of Chemical and Nuclear Engineering, University of California, Santa Barbara, CA, USA, 1995.
[11] K. Edsinger, G.R. Odette, G.E. Lucas, in: Proceedings of the IEA International Symposium on Miniaturized Specimens for Testing Irradiated Materials, KFA Julich, 22–23 September, 1994, 1995 p. 150.
[12] T.L. Anderson, Fracture Mechanics, CRC, Boca Raton, FL, 1995.
[13] C.F. Shih, J. Mech. Phys. Solids 29 (1981) 305.
[14] M. Nevaliainen, R.H. Dodds, Numerical investigation of 3-D constraint effects on brittle fracture in SE(B) and C(T) specimens, NUREG/CR-6317, US Nuclear Regulatory Commission, 1996.
[15] G.E. Lucas, G.R. Odette, J.W. Sheckherd, K. Edsinger, B. Wirth, in: 17th International Symposium, ASTM-STP 1270, ASTM, 1996, p. 790.
[16] G.R. Odette, E. Donahue, G.E. Lucas, J.W. Sheckherd, DOE/ER-0313/20, 1996, p. 11.
[17] E.G. Donahue, G.R. Odette, G.E. Lucas, these Proceedings, p. 637.
[18] G.R. Odette, DOE/ER-0313/20, US Department of Energy (1996) 283.
[19] G.R. Odette, G.E. Lucas, J. Nucl. Mater. 191–194 (1992) 50.
[20] E. Donahue, G.R. Odette, G.E. Lucas, J.W. Sheckherd, presented at the Eighth International Conference on Fusion Reactor Materials, Sendai, Japan, Oct. 1997.
[21] G.R. Odette, E. Donahue, G.E. Lucas, J.W. Sheckherd, in: 18th International Symposium on Effects of Radiation in Materials, ASTM STP-1325, ASTM 1997.
[22] D.J. Alexander, L.L. Snead, S.J. Zinkle, A.N. Gubbi, A.F. Rowcliffe, E.E. Bloom, DOE/ER-0313/20, 1996, p. 87.
[23] S.J. Zinkle, L.L. Snead, A.F. Rowcliffe, D.J. Alexander, L.T. Gibson, DOE/ER-0313/24, 1998, p. 33.
[24] D.J. Alexander, L.L. Snead, in: 18th International Symposium on Effects of Radiation in Materials, ASTM STP-1325, ASTM 1997.
[25] T.N. Baker, Yield, Flow, and Fracture of Polycrystals, Applied Science, Barking, 1983.